



Vancouver, Canada

May 31 – June 3, 2017/ *Mai 31 – Juin 3, 2017*

## APPLICATION OF A FOUR-BAR CRANK ROCKER MECHANISM AS A SUBTALAR JOINT LOADING SIMULATOR

Jn Baptiste, Jonelle<sup>1,8</sup>, Sabbagh, Joseph<sup>2</sup>, Andrews, Stephen<sup>3</sup>, Bowes, Julia<sup>4</sup>, Lou, Edmond<sup>5</sup>, Jomha, Nadr<sup>6</sup> and Adeeb, Samer<sup>7</sup>

<sup>1,2,3,4,5,6,7</sup> University of Alberta, Canada

<sup>8</sup> [jnbaptis@ualberta.ca](mailto:jnbaptis@ualberta.ca)

**Abstract:** The subtalar joint is responsible for inversion/eversion of the foot and ankle. Replacing subtalar joints damaged by primary osteoarthritis or sequelae of physical injuries with prostheses has not yet been studied according to literature. The standard method of treatment is subtalar joint fusion, where the joint tissues are removed and the talus and calcaneus bones are fused together to eliminate discomfort and improve the overall function of the foot and ankle. However, fusion eliminates inversion and eversion which is necessary for balancing the foot on uneven surfaces. Joint replacements have been successful in the hip, knee and ankle. Therefore, it may be possible to develop subtalar joint prostheses which maintain some degree of motion in addition to providing the benefits of fusion. The long term objective of this study is to develop and apply a testing protocol for wear of subtalar joint prostheses. No protocols exist for wear testing of ankle joints, so standards for wear testing of total hip-joint prostheses will be used as the basis for developing that of the subtalar joint. A four-bar crank rocker mechanism capable of applying a specific angular displacement to replicate eversion and inversion, +/- 10 degrees was designed. Cyclic loading of 50-800 N was applied using a fatigue testing machine. This simulator was optimized to withstand the applied fatigue loading without failure after a minimum of 5 million cycles. Furthermore, to simulate real-world conditions, the implants will be submerged in bovine serum diluted with deionized water during initial testing. While fatigue testing machines for implants exist, they are extremely costly in comparison to this apparatus which is an add-on to a regular fatigue testing machine. As experimental studies on subtalar joint prostheses have not yet been conducted, the results of this procedure will determine how the setup can be improved and which materials will be best suited for use as implants.

### 1. INTRODUCTION

Literature indicates that the use of subtalar joint prostheses is a novel approach. The main function of the subtalar joint is to assist the foot and ankle with stability on uneven surfaces and side-to-side motion, scientifically termed inversion and eversion. The subtalar joint is situated between the talus and calcaneus bones in the hind foot, below the true ankle joint. To date, the standard method of treatment available for severe injury to the subtalar joint is subtalar arthrodesis. With this procedure, the existing joint tissues are removed and the surfaces of the talus and calcaneus bones are conditioned to heal as a unit (American Orthopaedic Foot & Ankle Society, n.d.). While this procedure alleviates pain, it eliminates the articulation of the joint. There have also been successful cases of total joint replacement of the ankle (Prissell et al, 2017). Therefore, it may be possible for prostheses to maintain some motion in addition to alleviating the pain of injury to the subtalar joint. However, there are no standards for wear testing of ankle joint prostheses. The objective of this study is to design a flexible environment that subjects subtalar joint prostheses of various materials to double actuation.

Using the standards for wear of total hip-joint prostheses (ISO 14242-1 & 2), the test environment and parameters for practical loading and rotary displacement for the subtalar joint are defined. For total hip-joint replacement, the applied load in the hip is described by a fourth order polynomial ranging from 300-3000 N. The displacement follows a different sinusoidal curve for inward/outward rotation, abduction/adduction and flexion/extension (ISO 14242-2:2000). As aforementioned, the subtalar joint is mainly responsible for eversion/inversion, which is comparable to the inward/outward rotation of the hip joint. By replicating the surfaces of the talus and calcaneus bones, various materials for the wear testing of subtalar joint prostheses can be tested.

While machines specifically created for the wear testing of specific joints exist, this article focuses on a more cost effective option. One of the simplest devices used for controlling single degree of freedom (SDOF) motion is the four-bar mechanism. It can generate various types of motion such as rotation and sliding. By attaching a four-bar mechanism to an existing fatigue-testing machine, the prostheses may be subject to double actuation.

Finite element analysis is a versatile method that can be used to investigate the stresses generated in the four-bar mechanism due to the applied load on the prostheses. Since this is a dynamic model, varying stresses are expected along each linkage. Visual inspection of the largest difference between the minimum and maximum principal stresses along each linkage will be determined and compared with the fatigue limit of structural steel. In addition, the driving torque of the system under the specified loading can be obtained from FEA. Traditionally, a dynamic force analysis is performed to determine the driving torque of a four-bar mechanism. However, this is more tedious since the magnitude of the applied torque changes with the position of the linkages.

## 2. OBJECTIVES

Tailoring the requirements for the standards for wear of total hip-joint replacement to suit the subtalar joint, the objective of our work is to design a fatigue experimental setup with the following parameters:

1. Cyclic load of 50-800 N at 10 Hz to the talus jig (Figure 1)
2. Rotary displacement of  $\pm 10^\circ$  at 5 Hz to the calcaneus jig (Figure 2)
3. Totally submerge the prostheses in bovine serum diluted with deionized water
4. Test prostheses for wear every 1 million cycles, approximately 2.5 days, via inspection and the gravimetric method
5. Subject prostheses to a total of 5 million cycles

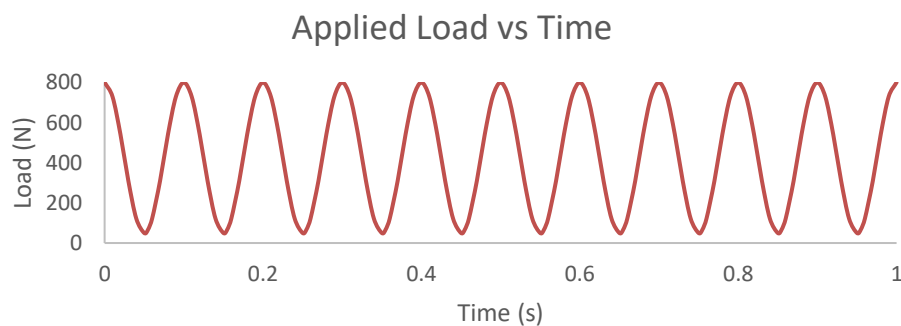


Figure 1: Applied Load to talus jig with time

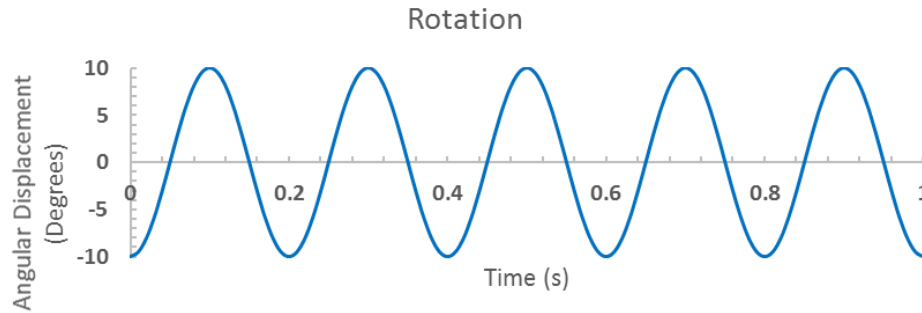


Figure 2: Angular displacement of calcaneus jig with time

### 3. METHODS

As this is a multidisciplinary project, the methodology is divided into the mechanical design aspect, which briefly summarizes the design of the most important components of this experimental setup, and the electrical aspect, which covers the power supply to the mechanical components.

#### 3.1.1 Experimental Setup - Mechanical

Based on the required simultaneous rotary displacement and cyclic loading, a device able to apply double actuation is required for this experiment. The concave and convex surfaces of the talus and calcaneus bones respectively are replicated by two jigs shown in Figure 3. Then, implants of various materials will be attached to the surfaces of these jigs and placed in contact with each other.

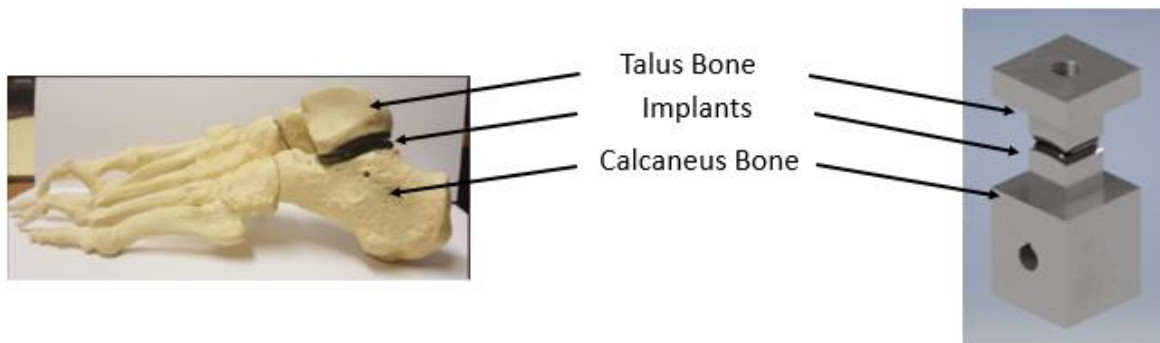


Figure 3: Experimental replication of the talus and calcaneus bones.

Cyclic loading of 50-800 N at 10 Hz is then applied by a fatigue-testing machine to the talus jig while the calcaneus jig undergoes inversion/eversion of +/- 10 degrees at 5 Hz. The frequency of the cyclic loading is doubled since this is a half-sine wave. Conveniently, the fatigue-testing machine is equipped with a water bath and the ability to adjust the temperature of the test fluid. This allows for the implants to be submerged in bovine serum diluted with deionized water as prescribed by the standards for wear of total hip-joint replacement prostheses [2].

Limitations for the design of the mechanism providing rotary displacement include the amount of space available and the ability to attach equipment to the fatigue-testing machine. To keep costs at a minimum, consideration is given to what is readily available on the market. Taking these limitations into account, multiple options were explored and a four-bar crank rocker mechanism was deemed as the best suited to meet the requirements of this experiment. By defining the required output angle of rotary displacement and other necessary parameters, a user is able to design a mechanism specifically tailored to his needs. The design of the four-bar mechanism used in this experiment is described further in section 3.1.3.

Figure 4 depicts the assembled model of the experimental setup in Autodesk Inventor. A motor drives the four-bar mechanism which is attached to a coupling. The inversion/eversion of the four-bar mechanism is then transmitted to the calcaneus block which is attached to the coupling by a shaft and key. This enables the precise rotation of the calcaneus jig with the four-bar mechanism. The surfaces of the implants are

frictionless so that rotation of the calcaneus jig will occur when the cyclic loading is applied through the talus jig as the two come into contact. The load cell is relocated to the top of the machine since it is not possible to attach the calcaneus jig to the bottom platen for this setup.

A mechanical lip seal was used to prevent leakage of the immersion fluid from the water bath and provide a frictionless surface for the shaft as it rotates. While the original fatigue-testing machine came with its own drainage system, multiple plates are stacked together to support the cantilever motor. Initially, fluid was able to seep through the gap in the top two plates and leak through the back of the plates. Therefore, silicon is used to seal off the spaces between the plates and allow the immersion fluid to flow straight through the existing drain. The plate from the existing machine used a face seal consisting of an O-Ring to prevent leakage from the water bath test chamber. Since the specifics of the O-Ring groove are not available and difficult to measure, the diameter and cross section of the O-Ring are used to replicate the original groove on the top plate to maintain this function.

Bolted connections are used to mount the plates and motor, while pins and screws are used to connect the linkages of the four-bar mechanism. Connecting multiple plates together with threaded bolts requires that through holes with a larger diameter be made on the top plates while threaded holes are made in the lower plates. This accounts for misalignment due to manufacturing and human errors.



Figure 4: Side and front view of the proposed experimental setup

### 3.1.2 Experimental Setup – Electrical

This experiment requires adjustable frequency for the four-bar mechanism to account for possible hindrances from voltage loss and the added pressure on the coupling from the immersion fluid. Therefore, an AC motor controlled with a variable frequency drive (VFD) is used for this experiment. AC motors are typically three phase while the building readily supplies single phase power. To overcome this, a VFD which feeds on single phase power but supplies three phase power is used. Furthermore, the motor is wired with a delta connection so that the phase and line voltages are equal (Electrical Technology, 2014).

In the future, the motor will be synched to the fatigue-testing machine so that double actuation is applied to the prostheses simultaneously.

### 3.1.3 Four-Bar Crank Rocker Mechanism

A four-bar crank rocker mechanism is one of the simplest means of controlling single degree of freedom (DOF) motion (Norton, 2004). This mechanism is a cheap and flexible alternative for this experiment since rotation is the only required DOF for the calcaneus jig. Figure 5(b) depicts the arrangement of the four-bar mechanism that is used in this experiment. In order for this mechanism to function, the Grashof condition described by equation 1 should be satisfied.

$$[1] s + l \leq p + q$$

Where:

$s$  = length of crank (mm)

$l$  = length of coupler (mm)

$p$  = length of rocker (mm)

$q$  = length of ground (mm)

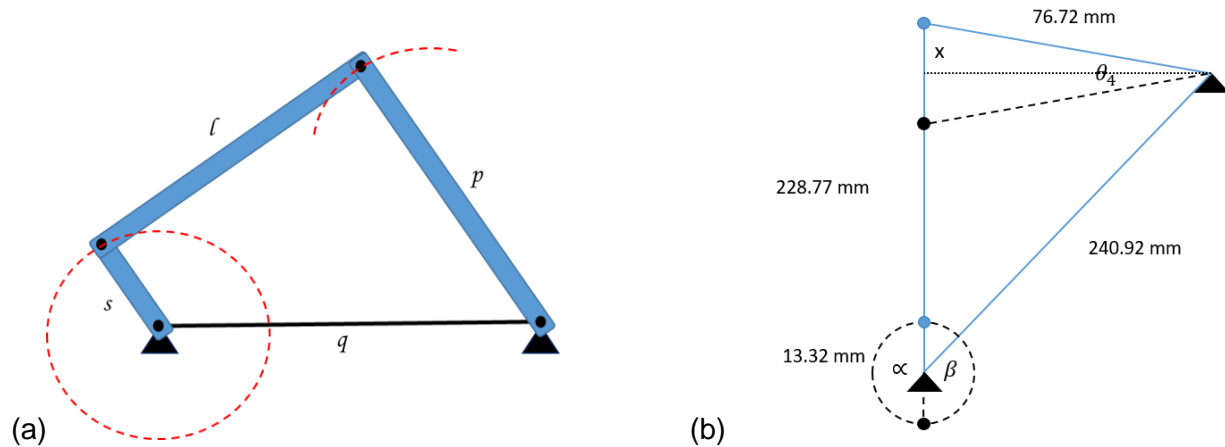


Figure 5(a) Typical four-bar crank rocker mechanism (b) Orientation of four-bar mechanism used in experiment

First the horizontal distance between the shaft and motor shaft is defined. Then, setting the output rocker angle,  $\theta_4$ , as  $20^\circ$ , the absolute value of the sum of the angles of eversion and inversion ( $10^\circ + -10^\circ$ ), the rocker length ( $p$ ) was determined. Using Pythagoras's Theorem to find  $x$  in Figure 5(b), the required crank length ( $s$ ) is then defined. Subtracting the length of the crank from the distance between the motor and shaft defines the coupler length ( $l$ ). The ground length ( $q$ ) is merely the distance between the two pinned ends and is not part of the physical linkages required for a four bar mechanism. As the crank makes a complete revolution, the rocker rotates between its minimum and maximum positions. The shortest linkage is replaced with a wheel since the fabrication of such a small piece is impractical. Constant speed is also required for the validity of this experiment, further rendering this mechanism as an even return four-bar crank rocker mechanism. In order to achieve constant speed, the angular displacement during the forward and backward motion,  $\alpha$  and  $\beta$  are made equal as shown in Figure 5(b).

#### 4. Finite Element Analysis

After the length of each linkage is established, a suitable cross section able to withstand a minimum of 1 million cycles and the input torque required to drive the system under the applied load are defined. While this can be determined using software that performs dynamic simulations, Finite Element Analysis (FEA) is more versatile and is performed using Abaqus/CAE 6.14-2.

##### 4.1 Model Parameters & Loads

Each linkage is modelled as a separate part in the  $+10^\circ$  displacement orientation of the four bar mechanism. Then, each part is defined as a beam element with a solid rectangular cross section (5 mm x 25.4 mm) and structural steel material properties defined in Table 1 prior to assembly. The nature of this experiment requires a dynamic explicit analysis requiring the need to define the density of the material and the use of amplitudes to define loads and displacements.

The applied cyclic load on the calcaneus/talus jigs is not directly applied at the pinned end of the rocker. In addition, it is assumed that the contact between the two oscillating implants will provide some friction that is required to be overcome by the motor. Therefore, using just a half sine wave of vertical pressure oscillating from 50 – 800 N is inaccurate for this analysis. To represent the effect of the applied load at the

pinned joint in a 2D analysis, the load is converted into a resultant moment. By setting the coefficient of friction ( $\mu$ ) as 0.3, the changing moment in time is calculated. Figure 6 depicts the amplitude of the applied moment with time, which takes into consideration the relative motion of the two rotating parts with respect to each other. It should be noted that the maximum moment applied at 0 seconds corresponds with the maximum position ( $+10^\circ$  rotary displacement) of the four bar mechanism.

Table 1: Material Properties

Property	Value
Young's Modulus, E	200 GPa
Density	7850 kg/m <sup>3</sup>
Poisson's Ratio	0.3

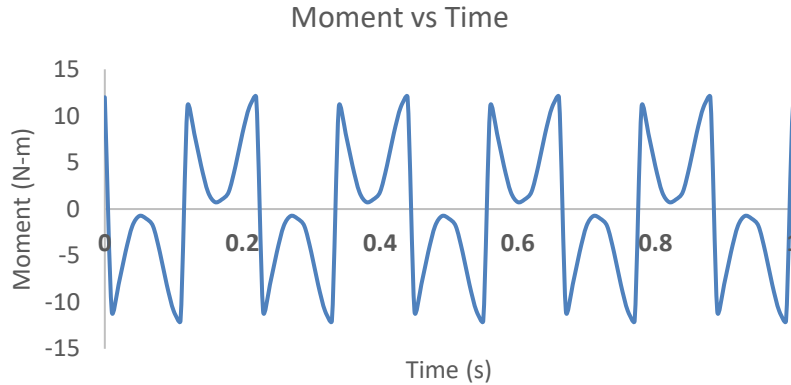


Figure 6: Graph of Moment Amplitude applied per second

In this experiment, the natural frequency,  $\omega$  of the system defined by Equation 2 is 10 Hz. This natural frequency is used to define the amplitude of rotation per second applied at the pinned end of the crank.

$$\begin{aligned}
 [2] \quad \omega &= 2\pi f \\
 &= 2\pi(5) \\
 &= 10\pi \text{ rad/s}
 \end{aligned}$$

where

$\omega$  = Natural Frequency (rad/sec)

f = Frequency (Hz)

Pinned connections are applied at the ends of the crank and rocker as shown in Figure 5(b). This is done by setting  $U1=U2=0$  under the Boundary Conditions module and is essential for the rotation of the crank. Tie constraints with untied rotational DOFs are then added at the two points connecting the linkages to each other. These constraints enable the crank to make complete revolutions while the rocker goes from its maximum to minimum positions. Adjusting the settings to record output every 0.01 seconds allows the user to see the mechanism rotating at the end of the analysis.

To account for the fatigue limit, the minimum and maximum principal stresses are recorded along each linkage. The input torque required to drive the system is determined by the reaction moment extracted at the pinned end of the crank.

## 4.2 Results

Taking the difference of the minimum and maximum principal stresses for each linkage is necessary to compare its fatigue limit to that of structural steel. These principal stresses are recorded at each node generated by the mesh in Abaqus along the length of each linkage. Based on the steady state values of Figures 7-9, the linkages are subject to very low minimum and maximum principal stresses ranging from 0 – 22 MPa while rotating and overcoming the applied torque. As expected, the rocker outputs the largest difference between the minimum and maximum principal stresses, approximately 22 MPa, since it is directly subject to the applied moment.

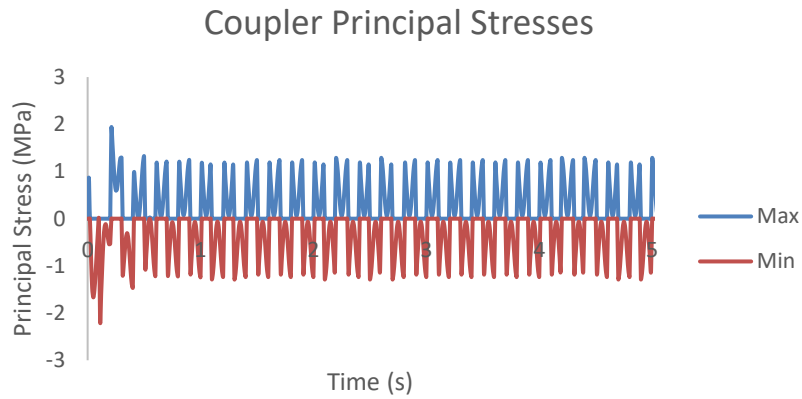


Figure 7: Coupler Principal Stresses

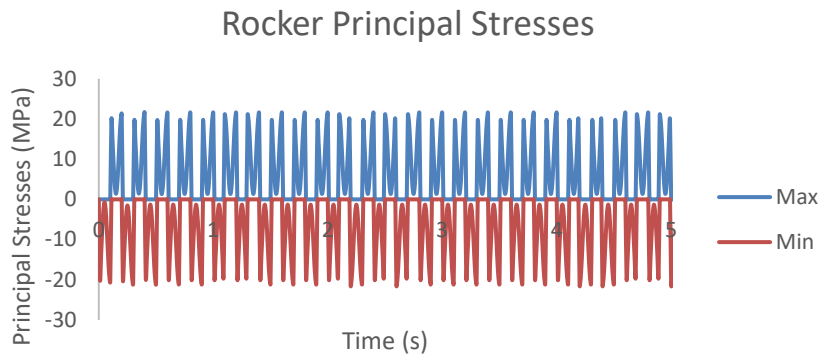


Figure 8: Rocker Principal Stresses

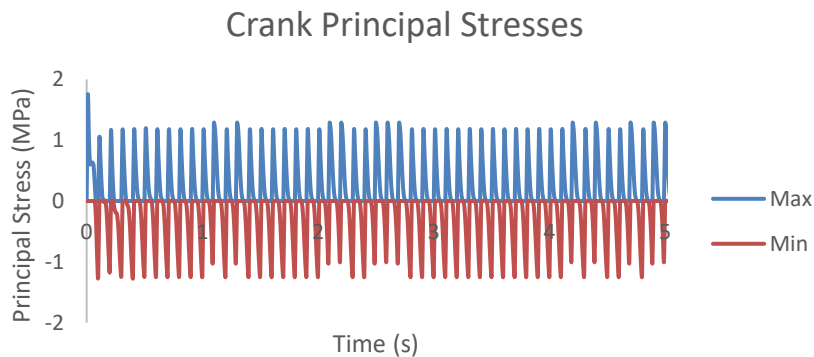


Figure 9: Crank Principal Stresses

The reaction moment depicted in Figure 10 is extracted at the pinned end of the crank since this area experiences the maximum stress from the applied moment. From the data, the highest peak occurs at 1.79 N-m and decreases to a steady state torque of approximately 0.9 N-m from 0.6 seconds. We are mainly interested in the steady state reaction moment since this experiment runs for approximately 2.5 days nonstop. For the motor to overcome the larger initial torque, the average of the steady state torque and initial torque, 1.33 N-m, is used.

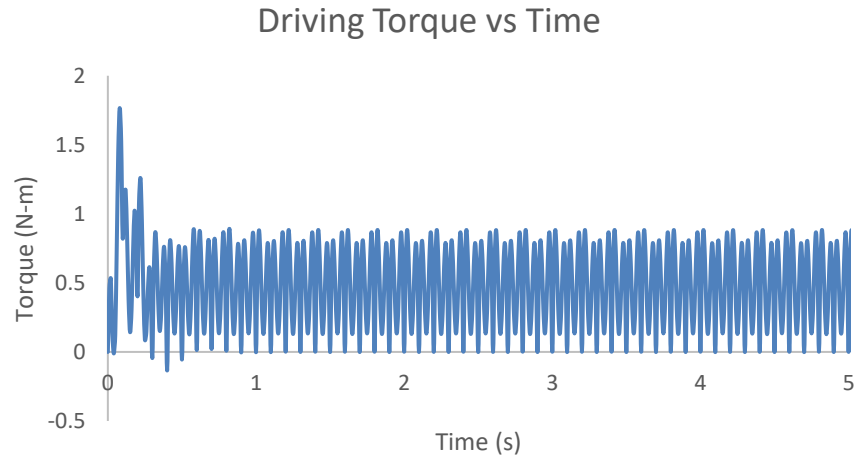


Figure 10: Required input torque of motor

Considering the additional forces that the motor may have to overcome, the average torque is considered to be 50% of what is required to drive the system. Equation 3 is used to calculate the size of the motor required.

$$\begin{aligned}
 [3] \text{ kW} &= \frac{2 \cdot 1.34102 \cdot \text{Torque (lb} \cdot \text{in)} \cdot f \cdot 60}{63,025} \\
 &= \frac{2 \cdot 1.34102 \cdot 1.33 \cdot 8.85074 \cdot 300}{63,025} \\
 &= 0.15 \text{ kW}
 \end{aligned}$$

where

f = frequency = 5 Hz

## 5. DYNAMIC FORCE ANALYSIS

To justify the initial input torque obtained from FEA, a dynamic force analysis is performed. A dynamic force analysis for a four-bar mechanism works by taking the sum of the forces and torques for each linkage to determine the driving torque of the system (Norton, 2004). Figure 11 depicts the parameters required for a dynamic force analysis of our system. This method works by considering the positions, lengths, mass, mass moment of inertia, velocity, acceleration, position vectors ( $r_{gi}$ ) for centre of gravity ( $CG_i$ ) and applied torque ( $M$ ) to calculate the driving torque ( $T_s$ ) of the system. Since the maximum torque (+/-12 N-m) is applied when the rocker is either at its minimum or maximum position respectively, the orientation of Figure 11 is used. Performing a dynamic force analysis in the position of maximum rotary displacement, the driving torque for the system in this position is 1.33 N-m.



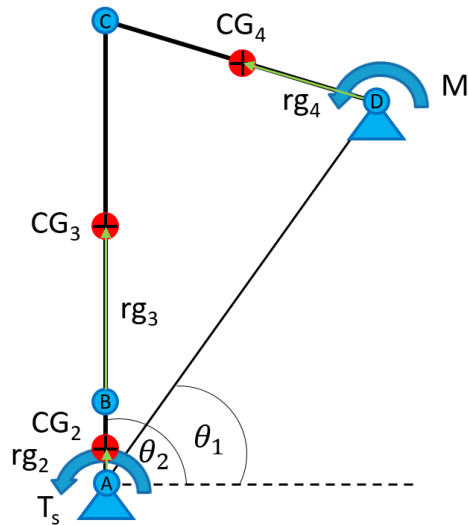


Figure 11: Parameters for a dynamic force analysis

## 6. ACTUAL EXPERIMENTAL SETUP

Figure 12 depicts the existing experimental setup. The blue pieces are 3D prints of the anticipated talus and calcaneus jigs, which are currently being manufactured. During the testing phase, the fatigue-testing machine will apply cyclic load through the shaft connected to the talus jig. As aforementioned, the crank is replaced with a round bushing. To the bottom right is the VFD connected to the motor. It is not yet synched to the fatigue-testing machine. Clamps successfully provide compression to the face seal for the water bath where the holes in the plates were too misaligned to be connected. A threaded bolt connects pieces to the top shaft. Until the jigs are manufactured, it is not possible to apply cyclic load to the mechanism as the talus jig is not securely connected to the top shaft.

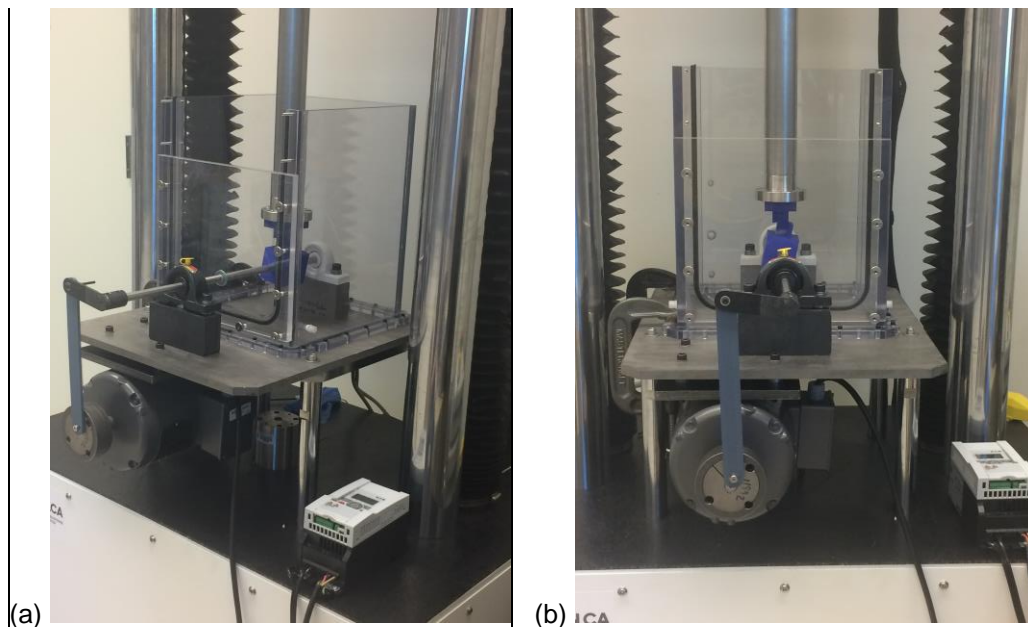


Figure 12: (a) Isometric view and (b) front view of experimental setup to date

## 7. CONCLUSION

Precision is a key factor to consider when manufacturing each mechanical component of this experimental setup. The manufacturing phase confirmed that a 3D model of an experimental setup is not enough to spot

unforeseen factors to consider during the design phase. Challenges encountered include leaks, misalignment of threaded holes between the stacked plates, misalignment of welded parts, unsatisfactory production of mechanical parts, errors in the precision of very small lengths and misshapen holes. When misaligned holes in stacked plates could not be remediated by drilling the threaded holes, smaller bolts were used. Regarding the electrical component of the setup, the wires connecting the VFD to the motor and the power cable should be properly crimped so that they do not fall out of place at any time and no power will be lost in transmission.

Structural steel has a fatigue limit of half of its ultimate tensile strength, approximately 225 MPa. The largest difference between the maximum and minimum principal stresses of the linkages, 22 MPa, is in the rocker. This value is approximately 10% of the fatigue limit of structural steel. Therefore, using 5 mm x 25.4 mm cross sections for the linkages will suffice for at least 1 million cycles in this experiment. The average torque from FEA matches the input torque obtained from a dynamic force analysis.

Attaching a four bar mechanism to an existing fatigue testing machine is a simple and inexpensive means of testing subtalar joint prostheses for wear. Based on FEA results, a 5 mm x 25.4 mm linkage cross section is sufficient for this experiment to run without failure from fatigue. In addition to this and accounting for efficiency, a 0.15 kW motor is sufficient to drive the system under the applied cyclic load.

### **Acknowledgements**

This research is partially funded by the Edmonton Orthopaedic Research Committee and NSERC. We would like to thank Andrew Wong, the University of Alberta Mec-E Shop, the I. F. Morrison Structures Lab, Carlos Darder and Stefan James for their significant contributions towards the technical aspects of this project.

### **References**

American Orthopaedic Foot & Ankle Society (n.d.). *Subtalar fusion*. Retrieved from <http://www.aofas.org/footcaremd/treatments/Pages/Subtalar-Fusion.aspx>

BS ISO 14242-2:2000 *Implants for surgery. Wear of total hip-joint prostheses. Methods of Measurement*. (2000). BSI Standards Limited.

BS ISO 14242-1:2014 *Implants for surgery. Wear of total hip-joint prostheses. Loading and displacement parameters for wear-testing machines and corresponding environmental conditions for test*. (2014). BSI Standards Limited.

Electrical Technology (2014). Comparison between star and delta connections. Retrieved from <http://www.electricaltechnology.org/2014/09/comparison-between-star-and-delta-connections.html>

Norton, R. L. (2004). *Design of machinery: an introduction to the synthesis and analysis of mechanisms and machines*. Boston: McGraw-Hill Higher Education, 2004.

Prissel, M. A., Hyer, C.F., & Berlet, G. C. (2017). A Review of 399 Total Ankle Replacements: Analysis of Ipsilateral Subtalar Joint Arthrodesis and Associated Talar Component Subsidence. *Journal Of Foot & Ankle Surgery*, 56(1), 10-14. Doi:10.1053/j.jfas.2016.10.004